Supporting information

Experimental Section

Synthesis of CeO_2 NRAs: All reagents used were of analytical grade and were used directly without any purification. In a typical synthesis process, the cathodic deposition was performed in a conventional three-electrode glass cell by galvanostatic electrolysis. A Ti foil of 1.5 cm × 3 cm and a graphite rod of about 4.0 cm^2 were used as working electrode and counter electrode, respectively. The reference electrode was an Ag/AgCl electrode. Prior to electrodeposition, the Ti foil was cleaned ultrasonically in distilled water, ethanol, and acetone and then rinsed in distilled water again. Three types of CeO_2 nanorods were electrodeposited on Ti substrates in solution of 10 mM $Ce(NO_3)_3$ + 50 mM KCl containing different concentration of NH_4Cl with a current density of 0.5 mA cm^{-2} for 120 min at 70 °C.

Characterizations: The as-synthesized products were characterized by field emission scanning electron microscope (FE-SEM, JSM-6330F), X-Ray Diffractometer (XRD, D8 ADVANCE), transmission electron microscopy (TEM, JEM2010-HR) and X-ray Photoelectron Spectroscopy (XPS, ESCALab250). The optical properties of the products were measured with a UV-Vis-NIR Spectrophotometer (UV, Shimadzu UV-3150). Raman spectroscopy was performed on a Laser Micro-Raman Spectrometer (Renishaw inVia) using a visible laser (λ= 514.5 nm) with an output laser power of 50 mW as the excitation wavelength at room temperature.

PEC measurements were carried out in a three-electrode cell with a flat quartz window to facilitate illumination of the photoelectrode surface. The working electrode is the CeO_2 film, while a graphite rod and a saturated Ag/AgCl electrode were used as counter and reference

electrode, respectively. A 1 M KOH and 1M CH_3OH mixture aqueous solution was used as the electrolyte. The illumination source was a 500W Xe arc lamp directed at the quartz photoelectrochemical cell. A water filter (2 M $NaNO_2$, absorb $\lambda < 390$ nm) was used to cut off the UV energy and avoid overheating. A 1 cm^2 region of the photoelectrode surface was illuminated with intermittent light exposure. The photocurrent densities were recorded with a CHI 750a electrochemical workstation (Chenhua, Shanghai) by using the difference between the light-off (dark current) and light-on currents acquired consecutively.

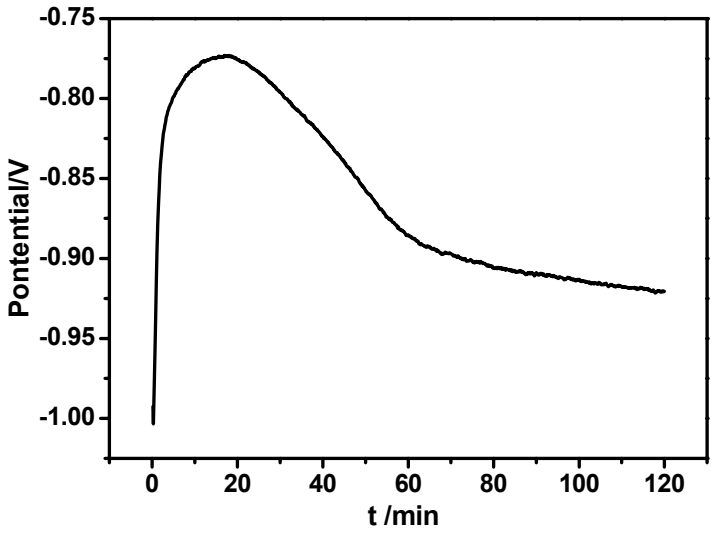

Fig. S1 Potential-time curve of the as-synthesized CeO_2 NRAs in solution of 10 mM $Ce(NO_3)_3$ + 50 mM NH_4Cl +50 mM KCl at 70 °C with a current density of 0.5 $mA \cdot cm^{-2}$.

For better understanding the growth mechanism of CeO_2 nanorods, we have investigated the formation process by the aid of the potential-time curve and controlled experiments with different deposition time. The potential–time curve of CeO_2 nanorods deposited with the current density of 0.5 $mA \cdot cm^{-2}$ at 70 °C is shown in Fig. S1. The potential first decreased rapidly in the initial stage of deposition and reached the minimum at 20 min, which indicates a fast process of nucleation and growth on Ti substrates.[1] Subsequently, the potential increased gradually between 20 and 60 min and then remained relatively stable. This variation can be attributed to the growth of nanorods, because the resistance increases with the growth of

product during this process. The growth rate of these nanorods was quick at the beginning and became slow with the deposition time advanced.

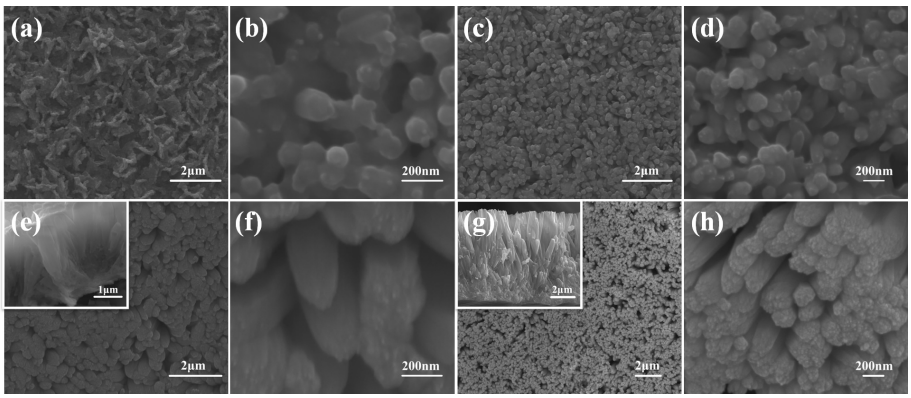

Fig. S2 SEM images of the as-synthesized samples after electrodeposition at 70 °C for: (a, b) 10 min; (c, d) 20 min; (e, f) 40 min; and (g, h) 80 min.

Fig. S2 displays the SEM images of the samples obtained at different reaction times. A layer of CeO_2 nanoparticles was first occurred after 10 min electrodeposition, as shown in Fig. S2a and b. These particles have a uniform diameter distribution about 150-180 nm. CeO_2 nanorods with a 150-180 nm diameter sprouted from the layer of CeO_2 nanoparticles when the electrodeposition time prolonged to 20 min, as shown in Fig. S2c and d. Vertical CeO_2 nanorods with diameters of 200 nm and lengths of 2.2 μm could be observed in Fig. S2e and f, when the reaction prolonged to 40 min. Further prolonging the electrodeposition to 80 min, high density nanorods were formed, as illustrated in Fig. S2g and h. The average diameter and length of these nanorods is about 200 nm and 6.1 μm, respectively. CeO_2 nanorods with diameters in the range of 200-230 nm and lengths up to 7.2 μm were formed after electrodeposition for 120 min. It is noted that the diameter of the nanorods is almost the same as that of the initial particles during the growth process, implying the particles are crucial for the final diameter size of the nanorods. Moreover, the length of the nanorods increased quickly from 20 to 80 min, resulting in the fast increase of resistance. Subsequently, the resistance increased slowly with the length of the nanorods. The results are in agreement with the variation of the potential-time curve.

On the basis of the above *E-t* curve analysis and SEM observations, the possible formation process can be defined as a seed-assisted electrochemical growth mechanism. The whole evolution process can be divided into three steps: (*i*) nucleation, (*ii*) formation of ceria seed

layer on the substrate, and (*iii*) further growth of NRAs on the seed layer. CeO_2 nuclei are firstly formed via electrochemical reactions, and the process can be described as follows: OH^- ions generate by electro-reduction of NO_3^- ions on the surface of cathode (Ti substrates). Then the OH^- ions react with Ce^{3+} and dissolved O_2 to form CeO_2. The whole procedures are expressed as eq. (1) and (2).

$$NO_3^- + H_2O + 2\,e^- \longrightarrow NO_2^- + 2\,OH^- \qquad (1)$$

$$4\,Ce^{3+} + 12\,OH^- + O_2 \longrightarrow 4\,CeO_2 + 6\,H_2O \qquad (2)$$

As the concentration of CeO_2 has reached supersaturation, CeO_2 nuclei form. Then the nuclei grow into a layer of CeO_2 particles as a seed layer for further growth of NRAs. With deposition time increasing, the nanorods gradually occur on the surface of the CeO_2 seed layer and finally form NRAs. In our case, these nanorods have a low crystallinity and a quasi-polycrystalline nature. However, it is still evident from the HRTEM and SEAD (Fig. 2b and c in the manuscript) that these nanorods grew along [110] direction. For the face-centered cubic CeO_2 crystal, the normal growth rates V of the three lowest crystallographic planes is $V_{(110)} > V_{(100)} > V_{(111)}$ because of the surface energy for the three planes is $\gamma\,\{111\} < \gamma\,\{100\} < \gamma\,\{110\}$.[2-3] Therefore 1D CeO_2 nanostructures such as nanorods,[3-4] and nanowires[5] are frequently acquired as they grow along the [110] direction.

[1] V. Tsakova, D. Borissov, S. Ivanov, *Electrochem. Commun*, 2001, **3**, 312.

[2] X. F. Tang, J. H. Li and J. M. Hao, *Materials Research Bulletin*, 2008, **43**, 2912.

[3] Z. L. Wang and X. D. Feng, *J. Phys. Chem. B*, 2003, **107**, 13563.

[4] P. X. Huang, F. Wu, B. L. Zhu, X. P. Gao, H. Y. Zhu, T. Y. Yan, W. P. Huang, S. H. Wu and D. Y. Song, *J. Phys. Chem. B*, 2005, **109**, 19169.

[5] Z. W. Zhang, C. G. Hu, Y. F. Xiong, R. S. Yang and Z. L. Wang, *Nanotechnology*, 2007, **18**, 465504.

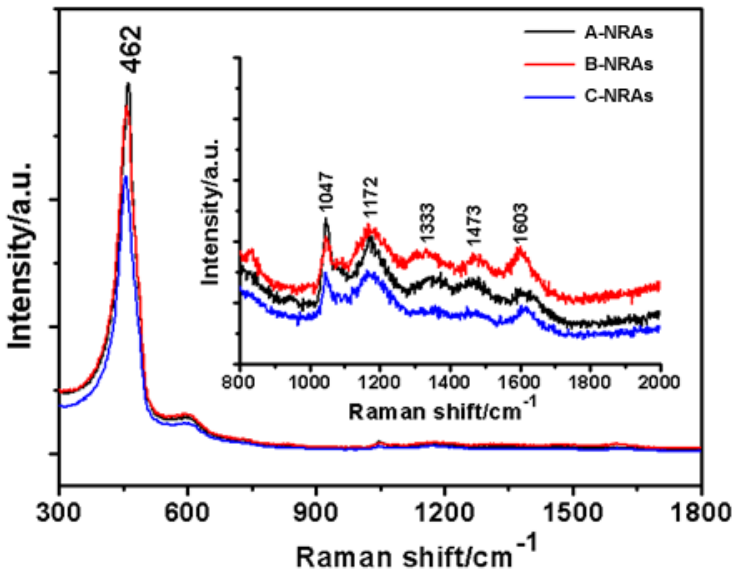

Fig. S3 Room temperature Raman spectra of the CeO_2 NRAs.

Raman scattering was used to characterize the surface defects of CeO_2 nanorods, and the typical Raman spectrums are shown in Fig. S3. The strong peak centered at about 462 cm^{-1} for the three samples is corresponding to the F_{2g} Raman active mode of CeO_2 cube structure.[1-2] From the Raman spectra at the wavenumber of 800 − 2000 cm^{-1} (inset in Fig. S3), five weak peaks located at 1047, 1172, 1333, 1472, and 1603 cm^{-1} from the CeO_2 nanorods can be observed clearly. The peak at 1047 cm^{-1} is attributed to the second-order Raman mode feature of peroxide adspecies (O_2^{2-}) and the weak peak at about 1172 cm^{-1} is assigned to the second-order Raman mode feature of surface superoxide species (O_2^-), which indicates the presence of oxygen vacancies. The peak at 1333 cm^{-1} might be ascribed to the third-order Raman active mode of F_{2g}.[2] Other two peaks at 1473 and 1603 cm^{-1} are not clear and possiblely derives from other structure of CeO_2 nanorods.

[1] J. E. Spanier, R. D. Robinson, F. Zhang, S. W. Chan and I. P. Herman, *Phys. Rev. B*, 2001, **64**, 245407.

[2] W. H. Weber, K. C. Hass and J. R. McBride, *Phys. Rev. B*, 1993, **48**, 178.

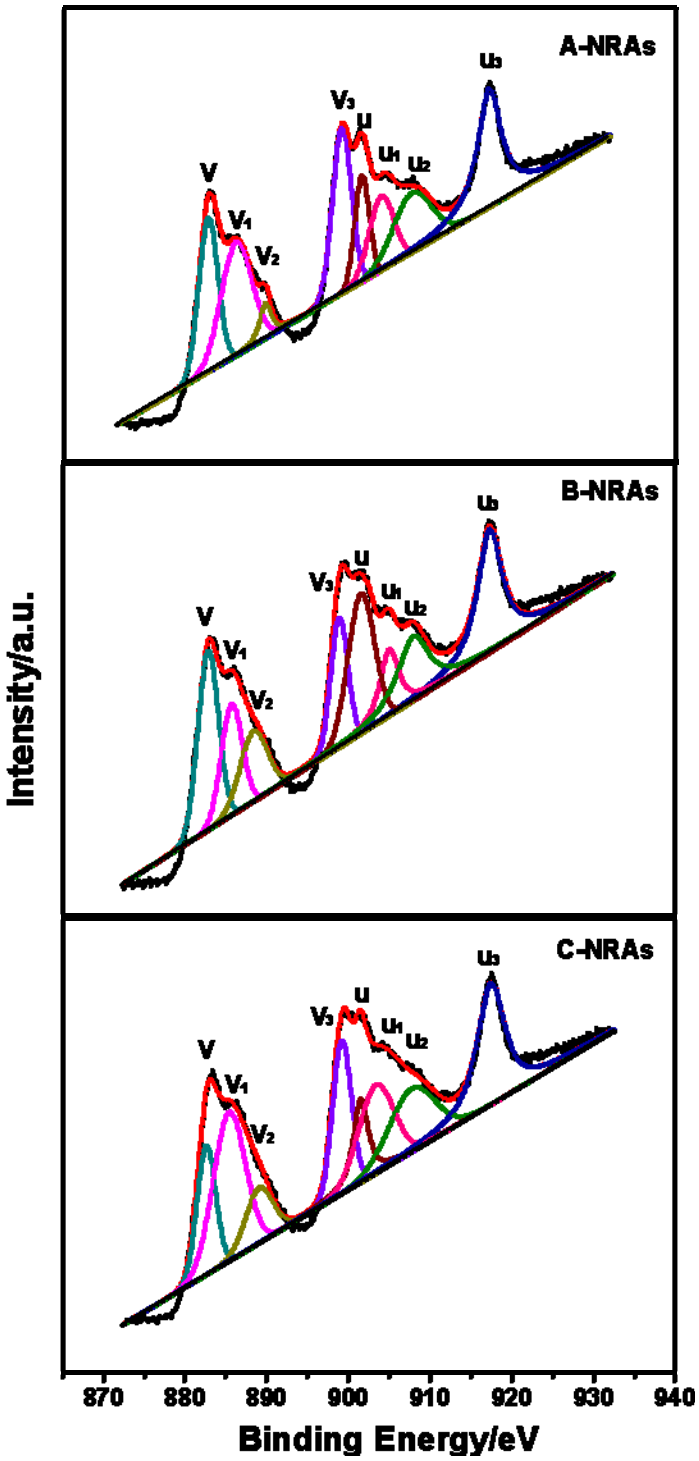

Fig. S4 Ce 3d spectra for the three types of CeO_2 NRAs.

XPS Ce 3d spectra for the three types of CeO_2 NRAs are presented in Fig. S4. Eight peaks are clearly observed in these spectra, which are labeled as u, u_1, u_2, u_3, v, v_1, v_2 and v_3. According to the literatures,[1-2] the peaks labeled as u, u_1, u_2 and u_3 refer to 3 $d_{3/2}$, while the peaks labeled as v, v_1, v_2 and v_3 refer to 3 $d_{5/2}$. The characteristic peaks of Ce^{4+} states are labeled as u, u_2, u_3, v, v_2 and v_3, respectively. The percentage of Ce^{3+} calculated from XPS

spectra in the deposits is about 4.93% for A-NRAs, 3.53% for B-NRAs, and 3.2% for C-NRAs, respectively.

[1] P. Burroughs, A. Hamnett, A.F. Orchard, G. Thornton, J. Chem. Soc., Dalton Trans. 1976, **17,** 1686.

[2] A. Q. Wang, P. Punchaipetch, R. M. Wallace and T. D. Golden, *J. Vac. Sci. Technol.*, *B* 2003, **213**, 1169.

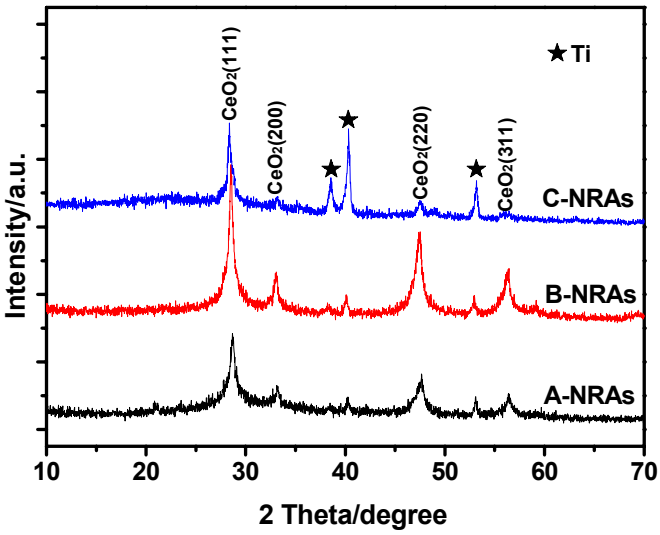

Fig. S5 XRD patterns of three CeO_2 samples.

Compared with bulk CeO_2, the adsorption bands of all the CeO_2 nanorod arrays exhibit a red-shift. Similar red-shift phenomenon, arising from the surface defects, has also been observed in some CeO_2 nanostructures.[1-6] Patsalas et al.[3-4] found that the E_g of CeO_2 film is red-shift with the increase of Ce^{3+} content and the enhancive localized states resulting from the defects is responsible for this red-shift. Chen et al.[5] reported that the E_g shifted toward short wavelength (blue-shift) with the decrease of Ce^{3+} content. For the three types of NRAs, clearly evidence of a great deal of defects is demonstrated by the HRTEM observations and Raman spectra (see the Fig. S3). The percentage of Ce^{3+} calculated from XPS spectra in Fig. S4 is

about 4.93% for A-NRAs, 3.53% for B-NRAs, and 3.18% for C-NRAs, respectively. On the other hand, it is well acknowledged that the E_g is strongly affected by quantum-size effect when the nanoparticle size is smaller than 10 nm, resulting in blue-shift.[6] The crystallite size of the CeO_2 samples calculated from (111) peaks in Fig. S5 by the Scherrer equation is 8.4 nm for A-NRAs, 12.2 nm for B-NRAs, and 14.5 nm for C-NRAs, respectively. Hence, based on the results above, we believed that the red-shift is mainly due to the surface defects.

[1] A. Corma, P. Atienzar, H. Garcia and J.-Y. Chane-Ching, *Nat. Mater.*, 2004, **3**, 394.

[2] C. Sun, H. Li, H. Zhang, Z. Wang and L. Chen, *Nanotechnology*, 2005, **16**, 1454.

[3] P. Patsalas, S. Logothetidis and C. Metaxa, *Appl. Phys. Lett.*, 2002, **81**, 466.

[4] P. Patsalas, S. Logothetidis, L. Sygellou and S. Kennou, *Phys. Rev. B*, 2003, **68**, 035104.

[5] M. Y. Chen, X. T. Zu, X. Xiang and H. L. Zhang, *Phys. B*, 2007, **389**, 263.

[6] Z. X. Li, L. L. Li, Q. Yuan, W. Feng, J. Xu, L. D. Sun, W. G. Song and C. H. Yan, *J. Phys. Chem. C* 2008, **112**, 18405.